Composite magnetic tunnel junctions for fast memory devices and efficient spin-torque nano-oscillators

Alexander Makarov, Viktor Sverdlov, Siegfried Selberherr
Institute for Microelectronics, TU Wien Gußhausstraße 27-29, 1040 Vienna, Austria

Abstract

We investigate a possibility to use composite magnetic tunnel junction structures (MTJs) to compose fast memory devices and efficient spin-torque nano-oscillators. In terms of magnetic memory, we study the switching statistics dependence on memory cell geometry by means of systematic micromagnetic simulations. We find that MTJs with a free layer composed of two ellipses with the axes $a/2 > b$ inscribed into a rectangle $a \times b$ demonstrate a substantial decrease of the switching time and the switching current as compared to conventional MTJs with a monolithic free layer. In terms of the spin-torque nano-oscillator we propose a novel structure based on two MgO-MTJs with a shared free layer. By performing extensive micromagnetic modeling, we found that the structure exhibits a wide tunability of oscillation frequencies from a few gigahertz to several ten gigahertz.

Keywords: magnetic tunnel junction, micromagnetic modeling, STT magnetic memory devices, STT nano-oscillators.

1 Introduction

New types of spintronics devices utilizing all-electrical magnetization manipulation by current, such as spin-torque transfer RAM (STT-RAM) and spin-torque nano-oscillators, have been intensely developed based on MgO magnetic tunnel junctions (MTJs) with a large magneto-resistance ratio [1]. Depending on the orientation of the magnetizations of the MTJ, the devices can be classified into two categories: “perpendicular” with out-of-plane magnetization direction and “in-plane” with magnetization lying in the plane of the magnetic layer. STT-RAM

WIT Transactions on Information and Communication Technologies, Vol. 49, © 2014 WIT Press
www.witpress.com, ISSN 1743-3517 (on-line)
doi:10.2495/ICIE130451

based on MTJs with perpendicular magnetization (p-MTJ) demonstrates a reduction of switching energy compared with that on in-plane MTJs, but still requires damping reduction and thermal stability increase [2]. Spin-torque oscillators based on MTJs with in-plane magnetization [3] show high frequency capabilities, but still need an external magnetic field and are characterized by a low output power level [4]. Oscillators on MTJs with perpendicular magnetization [5] and vortex-based oscillators [6] are shown to generate oscillations without external magnetic field, however, their low operating frequencies, usually below 2 GHz, limit their functionality and application as a tunable oscillator [4].

In the following, we demonstrate the potential of using composite structures for fast memory devices and efficient spin-torque nano-oscillators.

2 Model description

Our simulations of MTJs are based on the Landau–Lifschitz–Gilbert–Slonczewski (LLGS) equation describing the dynamics of the normalized magnetization $\mathbf{m}=\mathbf{M}/M_s$, where M_s is the value of the saturation magnetization in the free layer, in the areas of current flow [7]:

$$\begin{aligned}\frac{\mathrm{d}\mathbf{m}}{\mathrm{d}t} &= -\frac{\gamma}{1+\alpha^2}\cdot\Big((\mathbf{m}\times\mathbf{h}_{\mathrm{eff}})+\alpha\cdot\big[\mathbf{m}\times(\mathbf{m}\times\mathbf{h}_{\mathrm{eff}})\big]\\ &+\frac{g\,\mu_B\,j}{e\gamma M_s d}\cdot\Big(g(\theta_1)\cdot\big(\alpha\cdot(\mathbf{m}\times\mathbf{p}_1)-\big[\mathbf{m}\times(\mathbf{m}\times\mathbf{p}_1)\big]\big)\\ &-g(\theta_2)\cdot\big(\alpha\cdot(\mathbf{m}\times\mathbf{p}_2)-\big[\mathbf{m}\times(\mathbf{m}\times\mathbf{p}_2)\big]\big)\Big)\Big)\end{aligned} \tag{1}$$

and the Landau–Lifschitz–Gilbert (LLG) equation otherwise:

$$\frac{\mathrm{d}\mathbf{m}}{\mathrm{d}t}=-\frac{\gamma}{1+\alpha^2}\cdot\Big((\mathbf{m}\times\mathbf{h}_{\mathbf{eff}})+\alpha\cdot\big[\mathbf{m}\times(\mathbf{m}\times\mathbf{h}_{\mathbf{eff}})\big]\Big) \tag{2}$$

The definitions and values of the parameters used are standard and described, for example, in Ref. [11].

For the function $g(\theta)$ we use Slonczewski's expression for the MTJ with a dielectric layer [8]:

$$g(\theta)=0.5\cdot\eta\cdot\left[1+\eta^2\cdot\cos(\theta)\right]^{-1} \tag{3}$$

η is spin polarization factor, θ is an angle between the magnetization direction of the free layer and the pinned layer.

The local effective magnetic field is calculated as [9]:

$$\mathbf{h}_{\mathbf{eff}}=\mathbf{h}_{\mathbf{ext}}+\mathbf{h}_{\mathbf{ani}}+\mathbf{h}_{\mathbf{exch}}+\mathbf{h}_{\mathbf{demag}}+\mathbf{h}_{\mathbf{th}}+\mathbf{h}_{\mathbf{amp}}+\mathbf{h}_{\mathbf{ms}} \tag{4}$$

$\mathbf{h}_{\mathbf{ext}}$ is the external field, $\mathbf{h}_{\mathbf{ani}}$ is the magnetic anisotropy field, $\mathbf{h}_{\mathbf{exch}}$ is the exchange field, $\mathbf{h}_{\mathbf{demag}}$ is the demagnetizing field, $\mathbf{h}_{\mathbf{th}}$ is the thermal field, $\mathbf{h}_{\mathbf{amp}}$ is the Ampere field, and $\mathbf{h}_{\mathbf{ms}}$ is the magnetostatic coupling between the pinned layers and the free layer.

3 MTJs with a composite free layer

A penta-layer MTJ with a composite free layer (C-MTJ) was recently proposed [10] to improve switching characteristics of in-plane MTJs. The composite magnetic layer consists of two half-ellipses separated by a non-magnetic spacer (Figure 1b). The magnetization of the magnetic layers lies in-plane. The C-MTJs demonstrate a substantial decrease of the switching time and switching current as compared to the conventional MTJs with a monolithic free layer [11].

We perform a further structural optimization of C-MTJs (Figure 1b) by means of extensive micromagnetic simulations and propose a new structure, C2-MTJ (Figure 2c), with a free layer composed of two ellipses with the axes $a/2 > b$ inscribed into a rectangle $a \times b$. We compared the most important parameters of STT-MRAM devices, as switching time, thermal stability, and switching energy barrier with C2-MTJ and C-MTJ, conventional MTJ (Figure 2a), and M2-MTJ (Figure 2d) structure.

The simulations are performed for a nanopillar CoFeB/MgO (1 nm)/CoFeB/MgO (1 nm)/CoFeB MTJ, for a broad range of elliptical cross sections and different thicknesses of the pinned layers and the free layer. The other model parameters are: T=300 K, M_s=M_{sp}=8.9×10^5 A/m, A=1×10^{-11} J/m, K=2×10^3 J/m^3, α=0.005, and η=0.63 [12].

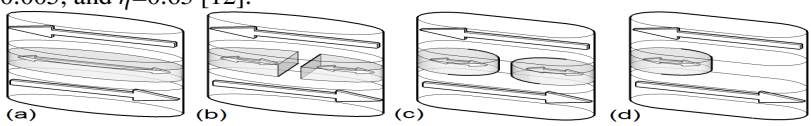

Figure 1: Schematic illustration of penta-layer MTJs with monolithic free layer (a) and M2-MTJ (d), and composite free layer C-MTJ (b) and C2-MTJ (c).

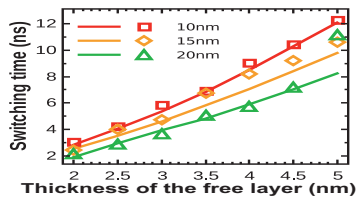

Figure 2: Switching time of C-MTJs (symbols) and C2-MTJs (lines) as function of the thickness of the free layer. The long axis is fixed at 52.5 nm and the thickness of the fixed layer is 5 nm. Dependences are shown for short axes of 10, 15, and 20 nm length. Each point is a result of statistical averaging with respect to 30 different realizations of the switching process.

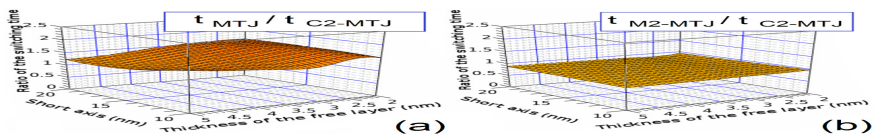

Figure 3: Ratio of the switching times in the monolithic structure and composite structure as function of thickness of the free layer and short axis length. The long axis is fixed at 52.5 nm. Dependences are shown for ratio: conventional MTJ vs. C2-MTJ (a), M2-MTJ vs. C2-MTJ (b).

3.1 Switching time

First, we study the switching times of C2-MTJs and compare it with those of C-MTJs. Our simulations demonstrate that C2-MTJs and C-MTJs have practically equal switching times for all considered cross-sections of the free layer (Figure 2).

The fact that the switching times in C-MTJs and C2-MTJs are equal must result in switching acceleration for C2-MTJs as compared to the conventional MTJ with a monolithic free layer. This is indeed confirmed by the results of our simulations shown in Figure 3a. Figure 3b demonstrates that C2-MTJs exhibit almost the same switching times as the structure with a single small ellipse (M2-MTJ, Figure 1d).

3.2 Thermal stability factor

We compare now the thermal stability factor for the two types of composite layer structures: C-MTJ and C2-MTJ. Figure 4 (left) confirms that the replacement of the free layer consisting of the two half-ellipses separated with a narrow gap (C-MTJ) by only two small ellipses (C2-MTJ), does not result in a loss of thermal stability. With 52.5×10 nm^2 cross section and 5 nm thickness of the free layer a thermal stability factor ~$60k_BT$ is obtained, which exceeds that of the single free layer p-MTJ demonstrated so far [13].

Next we compare the thermal stability factor for C2-MTJ with that of the two structures with monolithic free layer: conventional MTJ and M2-MTJ. Due to the removal of the central region from the monolithic structure the shape anisotropy in the C2-MTJ is decreased together with the thermal stability factor (Figure 4, right). The constant ratio of the thermal stability factor as a function of the aspect ratio and thicknesses of the free layer indicates that the thermal stability factors for both structures scales similarly. This means that in order to increase the thermal stability factor in C2-MTJs it is sufficient to increase the thickness of the free layer and/or the aspect ratio.

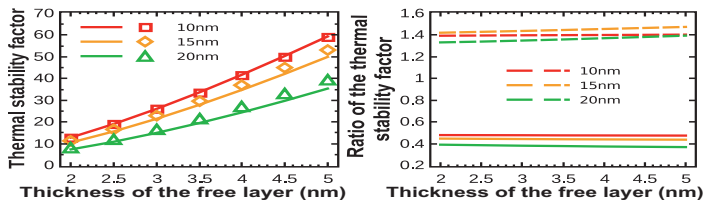

Figure 4: (left) Thermal stability factor for C-MTJ (symbols) and C2-MTJ (lines) as function of the thickness of the free layer. Each point is a result of statistical averaging with respect to 30 different realizations of the switching process. (right) Ratio of the thermal stability factors for monolithic structure and composite structure as function of thickness of the free layer and short axis length. Dependences are shown for ratio: M2-MTJ to C2-MTJ (solid lines), conventional MTJ to C2-MTJ (dotted lines). The long axis is fixed at 52.5 nm and the thickness of the fixed layer is 5 nm. Dependences are shown for short axes of 10, 15, and 20 nm length.

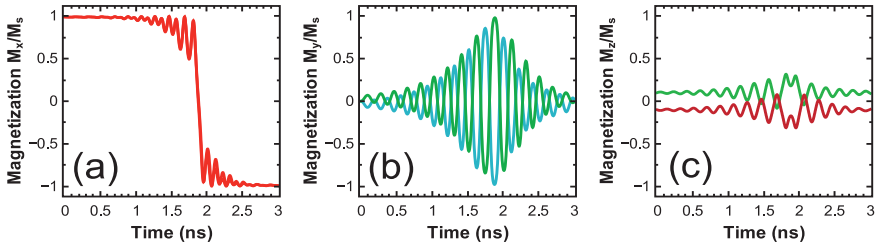

Figure 5: Magnetization components along the long axis (a), along the short axis (b), and along the axis perpendicular to the free layer (c) as a function of time for a MTJ element of 52.5×20 nm^2 size with a composite free layer (C2-MTJ). The magnetization of the left and right half is shown separately.

In comparison to the second structure with monolithic free layer, M2-MTJ, the C2-MTJ structure shows a gain in thermal stability by a factor of ~2 times (Figure 4, right), while maintaining the same switching time (Figure 3b), confirming the superiority of the C2-MTJ structure over the M2-MTJ one.

3.3 Switching energy barrier

To determine the reason of the fast switching in C2-MTJs we looked at the switching process in detail. Figure 5 shows that, as in a C-MTJ [11, 14], the switching processes of the left and right part of the C2-MTJ free layer occur in opposite senses to each other. Most importantly, the magnetizations of each piece stay in-plane. This switching behavior should lead to a decrease of the switching energy barrier. It turns out that the switching paths by current and due to thermal fluctuations are similar. Thus, as in p-MTJs, the switching barrier in a C2-MTJ

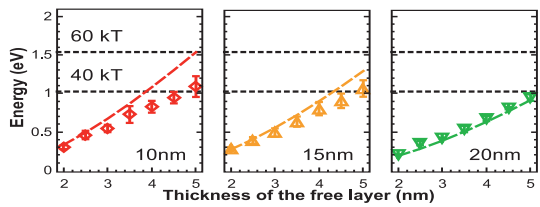

Figure 6: Thermal energy (lines) vs. switching energy (symbols) barriers for C2-MTJs. The long axis is fixed at 52.5 nm and the thickness of the fixed layer is 5 nm. Dependences are shown for short axes of 10, 15, and 20 nm length. Each point is a result of statistical averaging with respect to 30 different realizations of the switching process.

becomes practically equal to the thermal stability barrier defined by the shape anisotropy of the C2-MTJ free layer. Reduction of the switching barrier leads to the reduction of the switching time in a C2-MTJ as compared to a conventional MTJ at the same switching current density.

In the following, we compare the height of the thermal energy barrier with that of the switching energy barrier (Figure 6). As expected from the analysis of the

magnetization dynamics, the switching barrier becomes practically equal to the thermal stability barrier in C2-MTJ structures.

4 Spin-torque nano-oscillators

4.1 MTJs with a composite pinned layer

Now, we investigated a penta-layer MTJ structure with only half-elliptic pinned layers (Figure 7a). The simulations are performed for a nanopillar CoFeB (20 nm)/MgO (1 nm)/CoFeB (3.5 nm)/MgO (1 nm)/CoFeB (20 nm).

We find that the structure with half-ellipsis pinned layers develops stable oscillations with nearly constant amplitude. The Fourier transform of the signal is sharply peaked around the frequency ~6.785 GHz (Figure 7b). We note that the frequency of the oscillations only slightly depends on the current value (Figure 7c). This is due to the fact that despite the partial coverage of the free layer by the fixed layers, resulting in spin-current injection in only a part of the free layer, the free layer magnetization switching still occurs at a larger current densities limiting the range of current at which oscillations are observed.

4.2 Two MTJs with shared free layer

In order to prevent the switching of the free layer, thus improving an oscillatory behavior control, we have added the second MgO-MTJ to the system (Figure 8a). All the nanopillars used consist of CoFeB (5 nm)/MgO (1 nm)/CoFeB (3.5 nm)/MgO (1 nm)/CoFeB (5 nm) MTJs, with fixed layers 20×10 nm^2 (a×b)

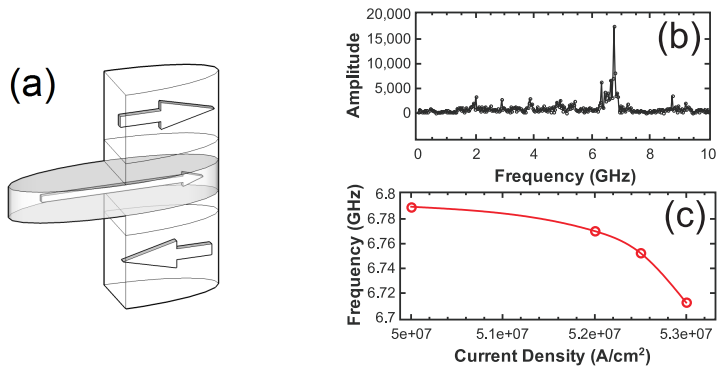

Figure 7: (a) Schematic illustration of a penta-layer MTJ with half-elliptic pinned layers. (b) The signal's Fourier transform for a current density 5×10^7 A/cm^2. (c) Frequency as function of current density.

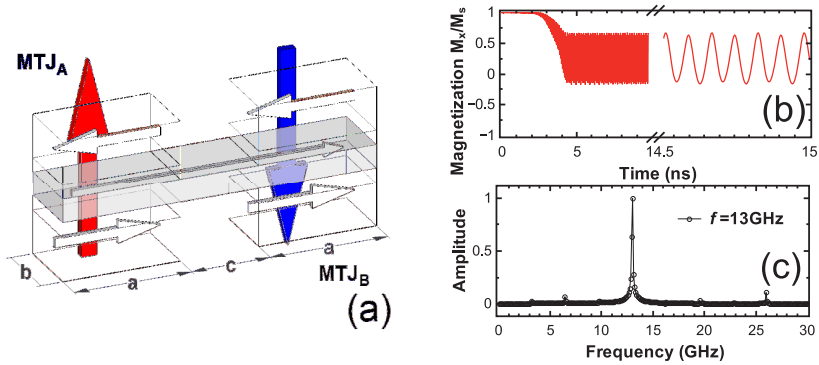

Figure 8: (a) Schematic illustration of a spin-torque oscillator based on two MgO-MTJs. Colored arrows indicate the positive direction of the current for each of the MgO-MTJs. (b) Magnetization x-component in MTJ_B as a function of time for a free layer of 50×10 nm^2. (c) Signal spectral density normalized to its maximum value. The current density through MTJ_A is 7.5×10^7 A/cm^2 and $1\cdot10^7$ A/cm^2 through MTJ_B.

and different free layer lengths. Figure 8b shows the switching process in such a structure in detail. We find that, in contrast to the previously considered case, the structure with two MgO-MTJs demonstrates stable oscillations with constant amplitude. The Fourier transform of the signal is sharply peaked around the frequency of 13 GHz (Figure 8c). Next, we studied the influence of the current density j_b/j_a ratio on the oscillation frequency (Figure 9). Increasing the ratio j_b/j_a increases the frequency (Figure 9, right).

5 Conclusion

We proposed and analyzed a new C2-MTJ structure with a composite free layer consisting of two ellipses with the axes $a/2$ and b inscribed into a rectangle $a \times b$.

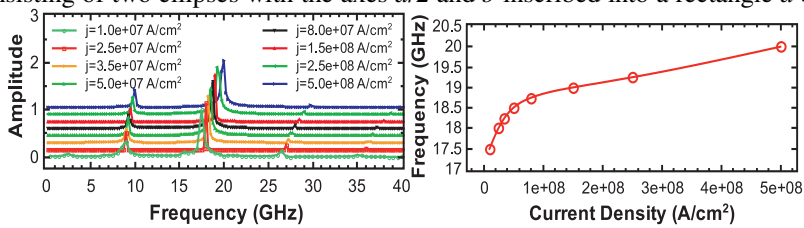

Figure 9: (left) Signal spectral density normalized to its maximum value. The length of the free layer is 60 nm (c=20 nm). Current density through MTJ_A varies from 1×10^7 to 5×10^8 A/cm^2, while in MTJ_B it is fixed to 5×10^6 A/cm^2. For convenience the curves are shown with 0.15 offset in the amplitude for different values of the current density through MTJ_A. (right) Frequency as a function of current density.

Our simulations show that, while preserving all the advantages of the C-MTJ structure, such as fast switching, high thermal stability factor, and very narrow distribution of switching times, the newly proposed structure can be easier fabricated, offering a greater potential for STT-MRAM performance optimization.

Furthermore, we proposed a new concept of spin-torque oscillators based on two MTJs with a shared free layer, which show stable oscillations without external magnetic field. The operating frequency of stable oscillations can be tuned in a wide range by varying the current densities flowing through the MTJs, making this structure attractive for many high frequency applications.

Acknowledgment

The financial support through the Grant #247056 MOSILSPIN by the European Research Council is acknowledged.

References

[1] A. Fukushima, T. Seki, K. Yakushiji, et al., *IEEE Trans on Magnetics*, **48**, p.4344, 2012.
[2] S. Ikeda, K. Miura, Y. Yamamoto, et al., *Nature Materials*, **9**, pp. 721–724, 2010.
[3] Z. Zeng, P. Upadhyaya, P. Khalili Amiri, et al., *Applied Physics Letters*, **99**, p. 032503, 2011.
[4] C.H. Sim, M. Moneck, T. Liewet, et al., *Journal of Applied Physics*, **111**, p. 07C914, 2012.
[5] Z. Zeng, G. Finocchio, B. Zhang, et al., *Scientific Reports*, **3**, p. 1426, 2013.
[6] A. Dussaux, B. Geordes, J. Grollier, et al., *Nature Commun.*, **1**, p. 8, 2010.
[7] A. Makarov, V. Sverdlov, D. Osintsev, et al., *IEEE Trans. on Magnetics*, **48**, p. 1289, 2012.
[8] J. Slonczewski, *Physical Review B*, **71**, p. 024411, 2005.
[9] A. Makarov, V. Sverdlov, S. Selberherr, et al., *Microelectron.Reliability*, **52**, pp. 628–634, 2012.
[10] A. Makarov, V. Sverdlov, D. Osinstev, et al., *Physics Status Solidi RRL*, **5**, pp. 420–422, 2011.
[11] A. Makarov, V. Sverdlov, S. Selberherr, et al., *Proceedings of IWCE*, pp. 1–4, 2012.
[12] M. Iwayama, T. Kai, M. Nakayama, et al., *Journal of Applied Physics*, **103**, p. 07A720, 2008.
[13] H. Sato, M. Yamanouchi, S. Ikeda, et al., *Applied Physics Letters*, **99**, p. 042501, 2011.
[14] A. Makarov, V. Sverdlov, S. Selberherr, et al., *Proceedings of SISPAD*, pp. 229–232, 2012.